ICARUS **99**, 273–288 (1992)

A Thermal Model for the Seasonal Nitrogen Cycle on Triton[1]

CANDICE J. HANSEN

Jet Propulsion Laboratory, California Institute of Technology, Pasadena, California 91109

AND

DAVID A. PAIGE

Department of Earth and Space Sciences, University of California, Los Angeles, Los Angeles, California 90024

Received March 4, 1992; revised July 10, 1992

A Mars thermal model has been adapted to study the seasonal nitrogen cycle on Triton. Unlike other models published to date, it incorporates diurnal and seasonal subsurface heat conduction, and accounts for the heat capacity of N_2 frost deposits. Key observables that this model attempts to reproduce include Triton's atmospheric pressure and surface albedo features at the time of the Voyager encounter, as well as changes in Triton's disk-integrated spectral properties between 1977 and 1989. Subsurface heat conduction is found to have an important effect on the behavior of Triton's polar caps and atmospheric pressure fluctuations. The results of this model differ from those of previous studies in that they generally do not predict the catastrophic freeze-out of Triton's atmosphere on a seasonal basis. The model results indicate that even for a wide range of possible input parameters, it is unlikely that Triton's bright southern polar cap is a seasonal nitrogen deposit, because it would have largely sublimated before the Voyager encounter. However, these results do not rule out the possibility of a large bright permanent polar cap in Triton's southern hemisphere. The best agreement between the model results and the available observations is obtained when Triton's seasonal nitrogen frost deposits are assumed to be darker than the underlying substrate. Assuming a constant nitrogen frost albedo of 0.62, a frost emissivity of 0.5, a substrate albedo of 0.8, and a substrate thermal inertia of 7×10^{-3} cal cm^{-2} K^{-1} sec$^{-1/2}$ yields good agreement with the surface pressure and global albedo patterns observed during the Voyager encounter, as well as a rapid change in disk-integrated albedo from 1977 to 1989 due to the retreat and disappearance of a dark south seasonal polar cap. These results lend support to microphysical arguments for the presence of dark, or smooth, translucent nitrogen frosts on the surface of Triton.

Presented at Neptune/Triton Conference in Tucson, Arizona, during January 6–10, 1992.

[1] The U.S. Government's right to retain a nonexclusive royalty-free license in and to the copyright covering this paper, for governmental purposes, is acknowledged.

INTRODUCTION

The Voyager observations of Neptune's moon Triton revealed a wide range of intriguing surface, atmospheric, and polar cap phenomena. Voyager gave us key data points vital to understanding the behavior of Triton's volatiles. The atmosphere is composed predominantly of N_2 (Broadfoot *et al.* 1989), the atmospheric pressure is approximately 1.6 Pa (Tyler *et al.* 1989), and images show a bright/dark boundary between the equator and 25° south latitude, which is taken to be the limit of a bright south polar cap (Smith *et al.* 1989) (see Fig. 1).

Early analysis of Triton observations led to the suggestion that Triton may be an example of a polar-cap-buffered surface/atmosphere system analogous to the CO_2 cap–atmosphere system on Mars (Trafton 1984). Ingersoll (1990) argued that many of the observable features on Triton's surface and atmosphere can be explained if Triton has an N_2 gas atmosphere in vapor pressure equilibrium with N_2 surface frosts.

Because Triton's frost properties are poorly constrained by observation or lab experiments, polar cap models are valuable tools for testing hypotheses regarding the physical properties of frosts on Triton. Two very different models for the behavior of seasonal nitrogen frost deposits on Triton were published shortly after the Voyager encounter. Stansberry *et al.* (1990) proposed a bright N_2 frost overlying a dark substrate, while Spencer (1990) proposed a dark N_2 frost overlying a bright substrate. Both models had only limited success predicting observed albedo features. The Stansberry *et al.* model predicted a bright southern polar cap extending from the south pole to 28° south latitude with a bright northern cap forming northward of the equator that was not observed in the Voyager images. The Spencer model predicted a dark north seasonal cap extending from the north pole to the

0019-1035/92 $5.00

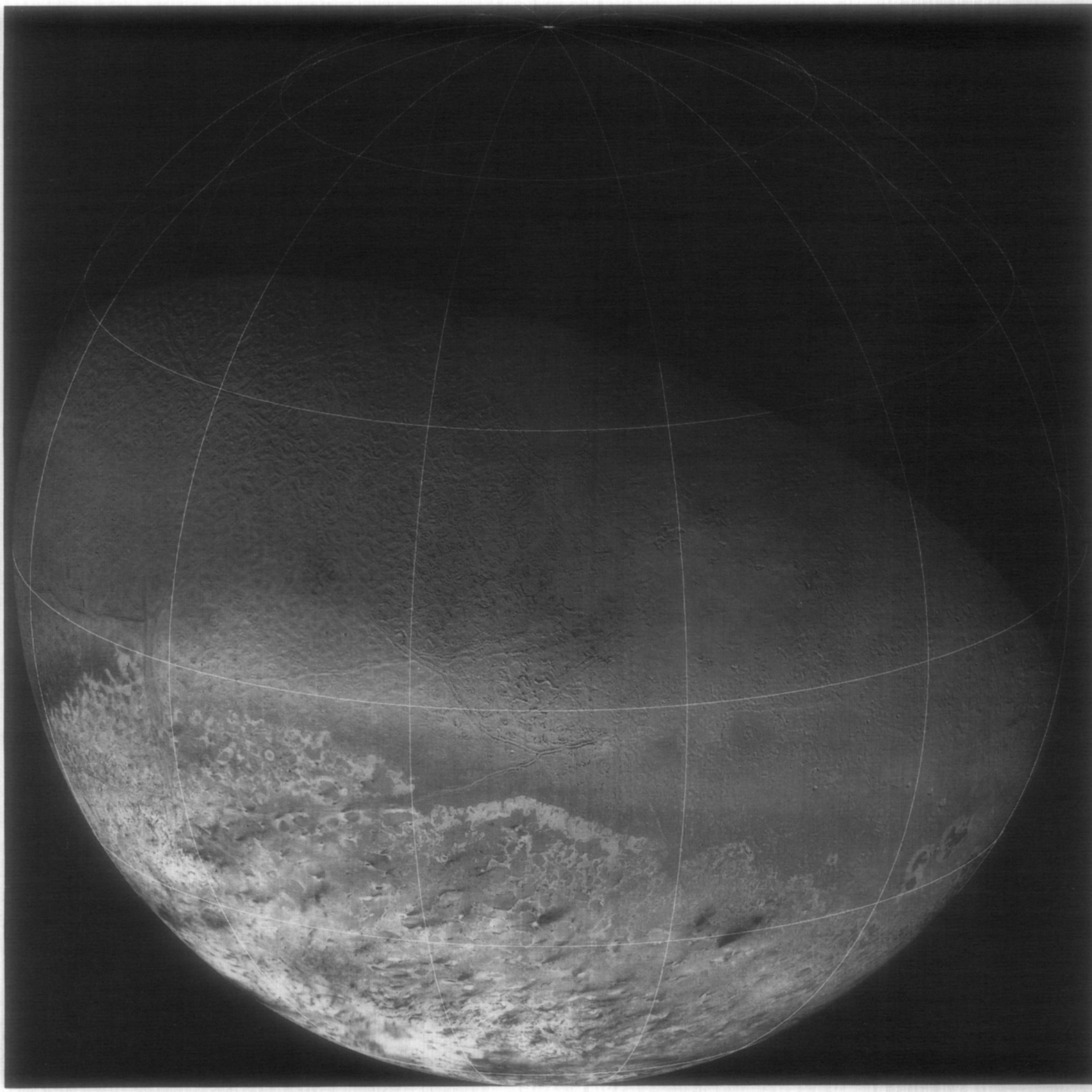

FIG. 1. Clearly visible in this image of Triton is the latitude of the boundary thought to mark the edge of the bright south polar cap. The equatorial region is also bright. North of the equator is a uniform, relatively dark region. The latitude of the subsolar point on Triton at the time of the Voyager flyby was $-45°$; thus the north polar region was in darkness, making it impossible to detect a potentially forming bright north polar cap. The authors thank Alfred McEwen who supplied this image, which he processed at the USGS, Flagstaff.

equator and a dark south seasonal cap extending from the south pole to 50° south latitude, which was also not observed in the Voyager images. Neither of these models incorporated the effects of subsurface heat conduction, which has been shown to be important when the behavior of the Martian seasonal polar caps is considered (Wood and Paige 1992).

In our study, we have taken advantage of the similarities between the seasonal cycles of CO_2 on Mars and of N_2 on Triton, and have modified a well-tested diurnal and seasonal Mars thermal model and applied it to conditions on Triton. The model takes into account insolation, infrared emission, subsurface heat conduction, latent heat, and phase equilibrium effects, to calculate surface and subsurface temperatures, frost condensation and sublimation rates, and atmospheric surface pressures as a function of local time and season. The primary questions we posed included:

1. Where are Triton's polar caps? The Voyager images show that bright deposits cover most of the southern hemisphere of Triton. Are these the seasonal nitrogen frost deposits, or are they lag deposits of solid methane or some other less volatile material? Will a model that includes the effects of heat conduction and other physical processes predict a phase lag for sublimation of the cap, that would allow a bright seasonal N_2 polar cap in the southern hemisphere to still exist at the time of the Voyager flyby?

2. Are Triton's seasonal caps bright or (relatively) dark? The two polar cap energy balance models published to date, Stansberry *et al.* (1990) and Spencer (1990), differ in their assumptions concerning frost albedo. Can we differentiate between these two models, or find criteria to test which assumption is in fact valid?

3. How do climatic conditions on Triton change with time? The Spencer (1990) model suggests that the atmospheric pressure on Triton fluctuates by many orders of magnitude seasonally—sometimes even condensing out entirely resulting in "catastrophic atmospheric freeze-out." Telescopic observations have given evidence for significant changes in the physical state or areal distribution of exposed methane on the surface (Cruikshank *et al.* 1989). Can this be reconciled with models for the transport and deposition of Triton's volatiles?

In the sections that follow, we describe the features of our Triton thermal model, present the results of a series of model runs, and finally, discuss the results in terms of the questions listed above.

THE MODEL

Our Triton thermal model is based on a modern-day Leighton and Murray (1966) diurnal and seasonal model that was originally developed to study the thermal behavior of the surface and subsurface of Mars (Paige 1992) and the Martian seasonal CO_2 cycle (Wood and Paige 1992, Paige and Wood 1992). Since all the model subroutines were written generically, the physics contained in the Mars model was easily transplanted to Triton. However, our early experiments showed that Triton cannot be treated as simply a cryogenic version of Mars, and significant changes would be required to model Triton's heat balance accurately.

The model is based on simple conservation of energy.

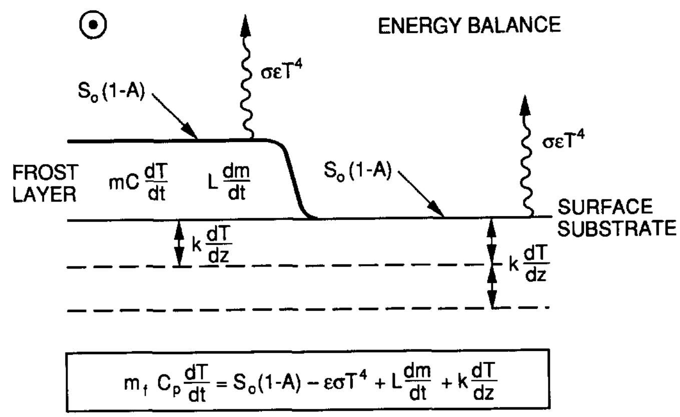

FIG. 2. This diagram illustrates all the terms in the heat balance equation for seasonal N_2 frost and bare soil in the Triton thermal model. Symbols are defined in the text.

See Fig. 2. Solar radiation is absorbed by the surface or frost in an amount dependent on albedo, infrared radiation is emitted, heat is conducted to and from subsurface layers, and latent heat and the heat capacity of the frost deposit control frost condensation and sublimation rates. The atmosphere is assumed to be transparent to radiation and atmospheric pressure is determined by subtracting the amount of N_2 condensed on the surface from the total N_2 inventory in the cap–atmosphere system. Nitrogen frost deposits are assumed to be isothermal, which in essence assumes that the deposit has sufficient porosity for its temperature to be controlled by vapor pressure equilibrium at all depths.

The model calculates diurnal and seasonal temperatures in the frost and at depth for a user-specified number of latitude bins and number of times per Triton hour. In order to speed up model runs (which require 3 days of clock time for the equivalent of 2100 Earth years) we used 18 equally spaced latitude bins and surface temperatures were calculated four times per Triton hour.

In the Triton model, N_2 is the dominant volatile species. Voyager observations revealed that Triton's atmosphere is composed predominantly of N_2, with CH_4, CO, and CO_2 as minor constituents (Broadfoot *et al.* 1989, Cruikshank and Apt 1984, Cruikshank *et al.* 1991). The Brown and Ziegler (1980) solid/vapor pressure equilibrium curve appropriate for Triton's low temperatures has been implemented in the model as a look-up table of temperature versus the natural log of pressure. Look-up table values reflect whether the N_2 phase is alpha or beta, but the small latent heat of the alpha–beta transition was not included. The latent heat of sublimation was fixed at 250,000 J/Kg for all temperatures (Brown and Ziegler 1980).

On Triton, calculating insolation rates is considerably more complicated than on Mars due to both Neptune's obliquity and the precession of Triton's inclined, retrograde orbit (Harris 1984). In the model we use the Trafton (1984) algorithm for Triton's subsolar latitude as a function of time.

Our model differs significantly from other Triton seasonal frost models published to date (Stansberry *et al.* 1990, Spencer 1990) in a number of respects. One is that we have incorporated heat flow from the interior. In the model runs presented here, the interior heat flow is assumed to be uniform over the entire globe. We used a heat flux of 0.006 W m^{-2} based on arguments for probable composition and radiogenic heat flow from the interior of Triton by Brown *et al.* (1991). Brown *et al.* (1991) show that uniform surface heat flow rates could change the surface temperature by 0.5 to 1.5 K, which could increase nitrogen partial pressure by a factor of 1.5 to 2.5.

Another important difference between our model and previous models is the consideration of thermal conduction into substrate soil layers. Layer thicknesses are calculated from the input parameters. The top three layers are set to be $\frac{2}{3}$ the depth of the diurnal thermal wave. Each subsequent layer is 1.13 times the thickness of the overlying layer. We use 60 layers to ensure coverage of the penetration of Triton's deep seasonal thermal wave. The time steps in the model and the top layer thickness are coupled—setting one determines the other by the relationship $(k\ dt)/(c\rho\ dz^2) < 0.25$, where k is the thermal conductivity, dt is the time increment, c is the specific heat, ρ is the density, and dz is the depth increment. This ensures numerically stable and accurate calculations of surface and subsurface temperatures (Clifford and Bartels 1986).

One fundamental difference between the heat balance of CO_2 frost deposits on Mars and the heat balance of N_2 frost deposits on Triton is the importance of the heat capacity of the frost deposits themselves. On Mars approximately 20% of the atmosphere condenses out on a seasonal basis. This corresponds to a change in frost point temperature of 1° out of an average surface temperature on Mars of 150 K, which makes the importance of frost heat capacity negligible. On Triton, earlier models (Spencer 1990) indicated that the entire atmosphere may condense out seasonally. For only a 100-fold reduction in atmospheric pressure, the frost point temperature decreases by 10°, a significant fraction of the average surface temperature, which is only 38 K (Conrath *et al.* 1989). On Triton, the heat capacity of the seasonal nitrogen frost deposits should buffer these dramatic changes. For example, to lower the temperature of 1000 kg of N_2 frost at ~40 K by only 1° requires approximately 10^6 Joules, or enough energy to sublimate approximately 6 kg of frost. Accounting for the heat capacity of the frost is necessary to correctly calculate partitioning of energy between frost deposit temperature changes and the amount of frost condensing or subliming, and should not be neglected as the atmosphere approaches complete freeze-out; otherwise, surface temperatures would plummet rapidly and energy would not be conserved. Since the magnitude of the heat capacity effect increases linearly with the mass of solid N_2 present, it is also likely to be of greatest importance when the potential stability of deep, permanent N_2 deposits is considered. In the model, the temperature-dependent solid N_2 heat capacities are determined from a lookup table using data compiled by Johnson (1960).

In our model, total energy is conserved locally, and the total mass of N_2 is conserved globally. The frost heat balance equation is

$$M_f C_p\, dT/dt = S_0(1 - A) - \varepsilon\sigma T^4 + L\, dm/dt + k\, dT/dz,$$

where:

M_f = Mass of N_2 frost deposit per square meter
C_p = Specific heat capacity of N_2 frost deposit
dT/dt = Rate of change of temperature of N_2 frost deposit
S_0 = Incident solar flux
A = Albedo of frost or substrate
ε = Emissivity of frost or substrate
σ = Stefan–Boltzmann constant
T = Temperature of frost or ground
L = Latent heat of N_2 frost condensation/sublimation
dm/dt = rate of N_2 condensation/sublimation per square meter
k = Thermal conductivity of substrate
dT/dz = Thermal gradient in uppermost layers of substrate.

Each time it is solved there are two unknowns, dm/dt and dT/dt. There is, however, one external constraint, which is that the frost be in solid–vapor equilibrium with the surrounding atmosphere. Therefore, at any given latitude or time, there is a unique combination of values for dm/dt and dT/dt such that the change in frost temperature, the amount of frost sublimed or condensed, and the frost point temperature that corresponds to the newly calculated atmospheric pressure are consistent with local conservation of energy and global mass conservation. In our model the correct combination of dm/dt and dT/dt are determined by trial and error. The solutions are bounded by two end-member cases: (1) all energy goes into changing the frost deposit temperature and no energy goes into sublimation/condensation of the frost (i.e., $L\, dm/dt = 0$), and (2) all energy goes into subliming/condensing frost and no energy goes into changing frost deposit temperature (i.e., $M_f C_p\, dT/dt = 0$). We then calculate the energy partition and atmospheric pressure for 18 intermediate evenly spaced cases and compare the results of each of the 20 cases to the average frostpoint temperature as determined from the calculated atmospheric pressure using the Brown and Ziegler vapor pressure curve. The best frost temperature/frost-point temperature match is selected, the amount of frost sublimed or condensed is added to or subtracted from the deposit, and the global atmospheric pressure is updated to reflect the amount of frost condensed or sublimed. This approach provides a seamless transition between the situation in which N_2 frost temperatures are determined primarily by solid–vapor equilibrium with N_2 gas, and the situation in which N_2 frost temperatures are determined primarily by radiation and conduction. This method was chosen over an iterative approach on the basis of speed and infallibility. A highly robust approach is required because of rapid changes in frost point temperatures that occur in just one timestep as the atmosphere approaches catastrophic freeze-out.

MODEL RUNS

Since first reporting our efforts (Hansen and Paige, 1991), we have made over 50 runs of the model. The first runs attempted to match results published previously to test the code. We verified the basic results of Stansberry *et al.* (1990) and Spencer (1990) by assuming negligible heat conduction, and also verified the magnitude of the effect of heat flow from Triton's interior on N_2 frost temperatures and surface pressures as reported by Brown *et al.* (1991). Then, we began to systematically explore parameter space to identify trends and to search for combinations of model input parameters that yielded results that agreed with the observables. All runs were initialized at 0 A.D. with no frost present at any latitude (the entire N_2 inventory is in the atmosphere).

The primary parameters that we varied were albedo and emissivity of the N_2 frost, albedo and thermal inertia of the substrate, and the N_2 total inventory. All of these parameters were assumed to remain constant with space and time within a run. Because the model considers only conservation of energy and heat balance, no explicit assumptions were made concerning variables such as frost grain size, grain metamorphism, permanent or temporary frost albedo variations, etc. Any or all of these possibilities could be evaluated with our model by judicious selection of input parameters. While it is true that these parameters may experience significant temporal variations on Triton, we felt that because of the exploratory nature of our study, it would be best to keep them constant with time for two reasons. First, we do not know what the average values of these parameters are, much less how they vary with time. Second, we did not feel that we could clearly identify trends and sensitivities by adding even more dimensions to our model parameter space.

TABLE I
Model Run Parameters

Run #	Thermal inertia ($\times 10^{-3}$ cal cm^{-2} K^{-1} sec$^{-1/2}$)	Albedo, ground	Albedo, frost	Emissivity, frost	N_2 inventory (kg/m^2)
1	1	0.8	0.62	0.5	200
2	1	0.8	0.62	0.5	20
8	30	0.8	0.62	0.5	200
13	3	0.6	0.85	0.2	200
14	3	0.6	0.85	0.4	200
15	3	0.6	0.85	0.6	200
16	3	0.6	0.85	0.8	200
18	6	0.6	0.85	0.4	200
21	3	0.8	0.62	0.2	200
22	3	0.8	0.62	0.4	200
23	3	0.8	0.62	0.6	200
24	3	0.8	0.62	0.8	200
30	1	0.6	0.85	0.4	100
31	7	0.6	0.85	0.4	100
32	1	0.8	0.62	0.5	50
33	7	0.8	0.62	0.5	50
34	50	0.8	0.62	0.5	50
35	20	0.6	0.85	0.4	100
53	1	0.8	0.62	0.5	100

Table I lists some of the parameter combinations we have investigated so far. In selecting albedo for the frost and ground we have concentrated on comparing a "bright" frost (albedo = 0.85) and a "dark" frost (albedo = 0.62), either of which is reasonable, based on analysis of the Voyager images (McEwen 1990). These two values allow us to compare the two previously published models (Stansberry *et al.* 1990, and Spencer, 1990). We have varied the frost emissivity from 0.2 to 1.0 to encompass the range of values that have been proposed in the literature (Stansberry *et al.* 1990, Nelson *et al.* 1990). We have varied the thermal inertia of the substrate from 0.3×10^{-3} cal cm^{-2} K^{-1} sec$^{-1/2}$, which would be appropriate for the surfaces of fine-grained icy satellites (Morrison and Cruikshank 1973) to 50×10^{-3} cal cm^{-2} K^{-1} sec$^{-1/2}$, which would be appropriate for solid water ice. We have also varied the total N_2 inventory from 20 to 200 kg/m$^{\wedge 2}$, globally averaged, which is a reasonable range of values considering cosmic abundances and the observed strength of the N_2 absorption feature (Cruikshank *et al.* 1984).

Figure 3 (run #33) is an example of the model's output. All parameters are shown as a function of time from the year 0 AD to the year 2100 AD. The top panel shows the "whole disk albedo," here calculated by integrating the fractional coverage of frost and bare ground that would be visible from the earth at that year. If the spectral properties of these surfaces were known then these whole

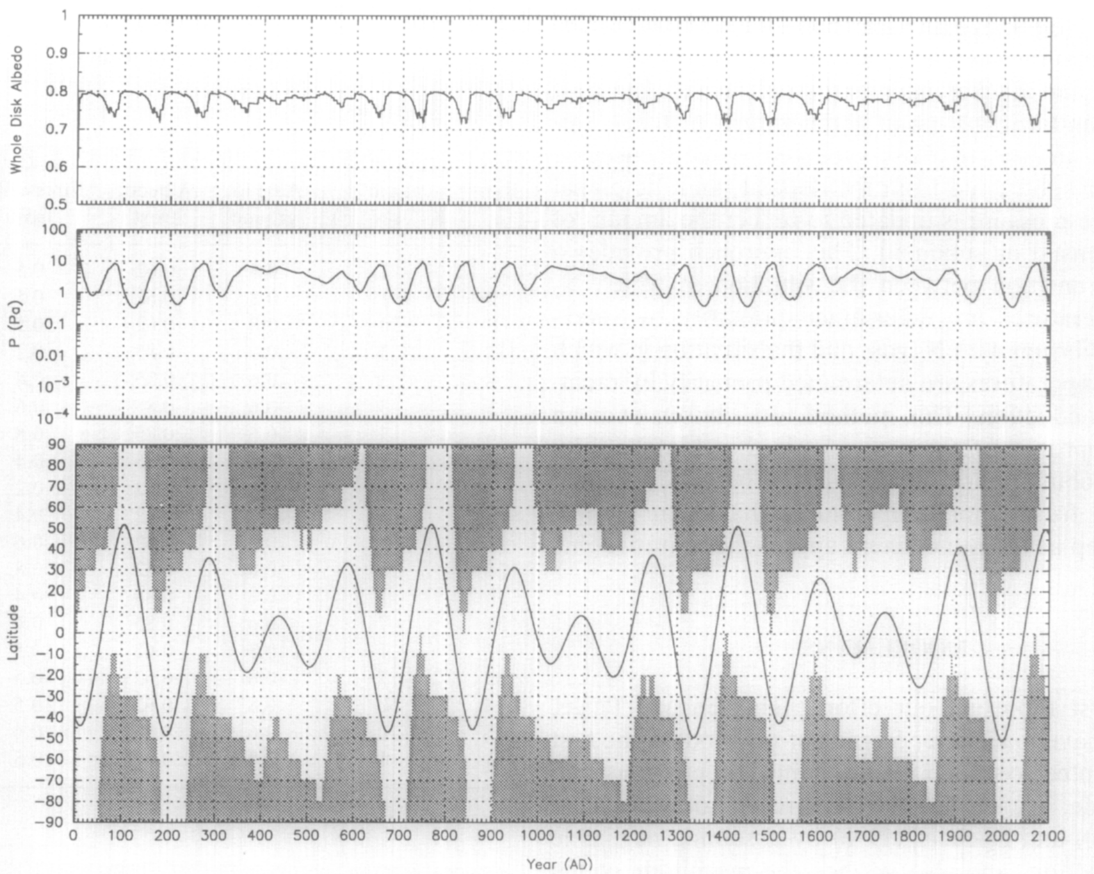

FIG. 3. Model results for run #33 with "dark" frost (albedo = 0.62), emissivity = 0.5, thermal inertia = 7×10^{-3} cal cm^{-2} K^{-1} sec$^{-1/2}$, and N_2 inventory = 50 kg/m^2. This set of parameters has produced the best fit so far to the albedo boundaries and atmospheric pressure at the time of the Voyager flyby. All parameters are shown as a function of time from the year 0 AD to the year 2100 AD. The top panel shows the "whole disk albedo," here calculated by integrating the fractional coverage of frost and bare ground that would be visible from the earth at that year. The middle panel plots atmospheric pressure as a function of time on a log scale. The bottom panel shows the locations of frost deposits and bare substrate as a function of time. The stippled areas are the latitudes that are covered by frost at noon local time. The solid line shows the latitude of the subsolar point.

disk albedos could be interpreted as color variations. The middle panel plots atmospheric pressure as a function of time on a log scale. The bottom panel shows the locations of frost deposits and bare substrate as a function of time. The stippled areas are the latitudes that are covered by frost at noon local time. The solid line shows the latitude of the subsolar point.

RESULTS

Model runs so far have yielded interesting results, both for identifying and understanding trends, and for making absolute judgements concerning possible states of Triton's polar caps. The major trends that have been identified are as follows:

Emissivity Variations

Frost deposition patterns are markedly different for bright vs dark frost cases as the frost emissivity is varied. Figure 4 shows the results of runs 14 and 16, which are "bright frost" runs, compared to runs 22 and 24, which are "dark frost" runs. Emissivities of 0.4 and 0.8 are compared within the albedo subset (Fig. 4a vs Fig. 4b and Fig. 4c vs. Fig. 4d). High emissivity (0.8) bright frost clears frost from the equatorial zone while low emissivity (0.4) bright frost still covers equatorial regions seasonally. In contrast high emissivity dark frost shows just the opposite behavior, deposition in equatorial regions, while low emissivity dark frost moves toward the poles. These results suggest that the sizes of Triton's seasonal polar caps are determined by the difference between global frost point temperatures and equatorial surface temperatures. This is because a high emissivity bright frost will be very cold, thus unstable at the equator. Low emissivity bright frost and high emissivity dark frost represent intermediate energy cases, not greatly different in temperature from the equatorial regions. The low emissivity dark frost should be warmest of all, but in this case most of the nitrogen is in the atmosphere, not condensed on the ground.

It is apparent in the results presented in Fig. 4 not only that increasing N_2 frost emissivity leads to decreasing atmospheric pressure for both the "bright" and "dark" frost cases as has been discussed by other authors (Stansberry *et al.* 1990, Nelson *et al.* 1990), but also that the high emissivity cases have the most pronounced seasonal atmospheric pressure fluctuations.

Subsurface Heat Conduction

For both "bright" and "dark" frost, increasing the thermal inertia of the ground prevents frost accumulation in the equatorial regions. This occurs for two reasons. First, on a seasonal time scale, higher thermal inertia surfaces require longer to cool off or to warm up, thus remain closer to their annual average temperatures. Second, surfaces with higher thermal inertias have higher annual average temperatures (Paige 1992). Figures 5a and b compare two identical bright frost cases (runs #30 and #35) with a factor of 20 difference in thermal inertia. This trend is most pronounced for bright frost.

High thermal inertia also tends to smooth seasonal atmospheric pressure fluctuations as can be seen in Figs. 6a and b (dark frost runs #32 and #34). This would be due to the tendency of high thermal inertia surfaces to change temperature less rapidly, causing the temperature of the ground in contact with the frost deposit to be very stable. The heat capacity of the frost deposit itself has a similar, though much less significant, influence on atmospheric stability.

Seasonal subsurface heat storage is likely to be important when north–south asymmetries in the stability of permanent N_2 polar caps are considered (Spencer and Moore 1992), as has been noted for Mars (Jakosky and Haberle 1990). On Mars, where the substrate is darker than the frost, if formerly frost-covered ground is exposed in the summer it may warm up sufficiently to prevent recondensation of frost the following winter. The results of Fig. 4c suggest that on Triton exposure of the substrate may not prevent the reformation of a permanent N_2 polar cap if the albedo of the substrate is higher than the albedo of the frost.

N_2 Inventory

The appearance of permanent polar caps, which is determined by the annual heat balance at the poles, stabilizes atmospheric pressure. If a permanent cap is present, adding to the N_2 inventory does not change atmospheric pressure; rather, it adds to the cap frost deposit depth. Figure 7 compares the results of run #18, which had a N_2 inventory of 200 kg/m^2, with run #31, which had 100 kg/m^2.

If permanent caps are not present, increasing the total N_2 inventory raises the global atmospheric pressure. This effect has also been reported in a study of the seasonal polar caps on Mars (Wood and Paige, 1992). Figure 8 compares the results of run #2, 20 kg/m^2, with run #53, 100 kg/m^2.

Examination of the results of all the model runs shows that for some of the cases, it may have been desirable to perform calculations for much longer than the equivalent of 2100 Earth years. Cases that did not include permanent N_2 polar caps appear to have completely equilibrated by the end of the calculations, whereas cases that did include permanent N_2 polar caps appear to still be slowly converging. This is primarily due to the fact that near the poles, annual averaged insolation rates are not strong functions of latitude. This suggests that the calculated atmospheric pressures for these cases are close to their equilibrium values, whereas the calculated cap boundaries near the permanent caps may not be at their final equilibrium positions. Previous considerations of buffered cap–atmosphere systems have indicated that in true equilibrium, permanent polar caps should only be stable at the exact location where the annual heat balance is most favorable, which in this model would be the geographic poles (Murray and Malin 1973, Spencer 1990). The results of the calculations presented here indicate that on Triton, the timescales required to achieve this final equilibrium state may be sufficiently long that other factors not considered in this model such as viscous spreading (Kirk and Brown 1991) or slopes (Yelle 1992) may be important for determining the ultimate spatial extents of permanent N_2 polar caps on Triton.

DISCUSSION

In general, it appears to be much easier to use this model to match the atmospheric pressure observed on Triton at the time of the Voyager flyby than it is to match the observed albedo boundaries. In order to match the atmospheric pressure, it is only necessary to vary one of the frost's radiative properties such as emissivity once permanent polar caps are established. If permanent polar caps are not established, judicious adjustment of the N_2 inventory also makes it possible to arrive at agreement to the observed value.

In contrast, it is very difficult to produce an albedo boundary at ~5° south latitude with this model. For the bright frost case, a seasonal cap cannot be produced that matches the observables. We had posed the hypothesis that the south polar cap was seasonal N_2, with a phase lag in its sublimation due to subsurface energy storage that would allow its existence even in late spring in the southern hemisphere. Increasing the thermal inertia of the substrate does not result in a phase lag in the sublimation of a bright south seasonal cap, however, but rather drives

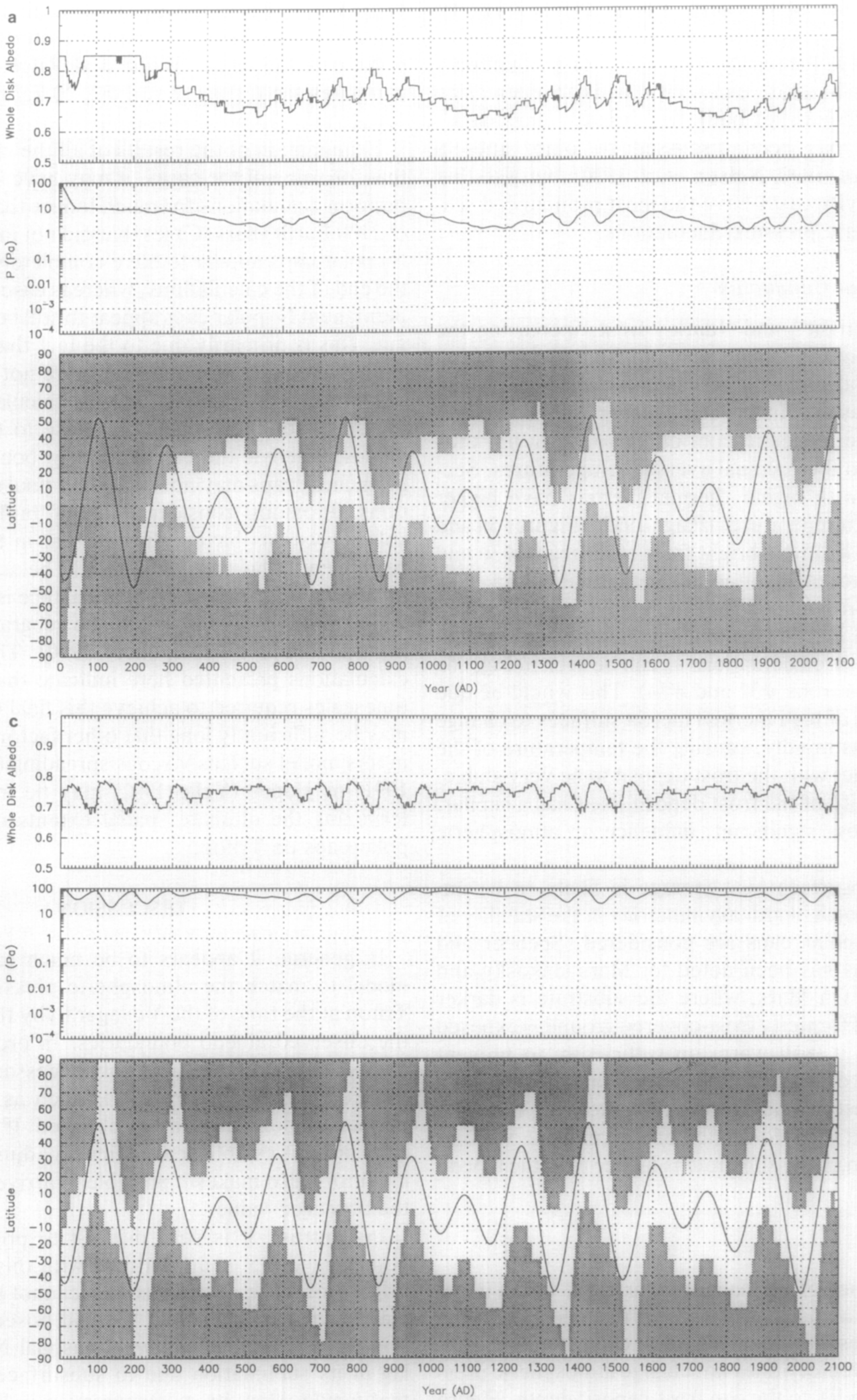

FIG. 4. These panels contrast frost deposition patterns and atmospheric pressure as a function of frost emissivity and albedo. Panels a and c are low emissivity cases (emissivity = 0.4) with a "bright" frost (a) and a "dark" frost (c), run #14 and run #22, resp. Panels b and d are higher emissivity (emissivity = 0.8) runs, again contrasting bright frost (b) vs. "dark" frost (d), run #16 and run #24, resp. These results show that frost emissivity affects polar cap boundaries differently, depending on frost albedo. Thermal inertia was held constant at 3×10^{-3} cal cm^{-2} K^{-1} sec$^{-1/2}$, and the N_2 inventory was 200 kg/m^2.

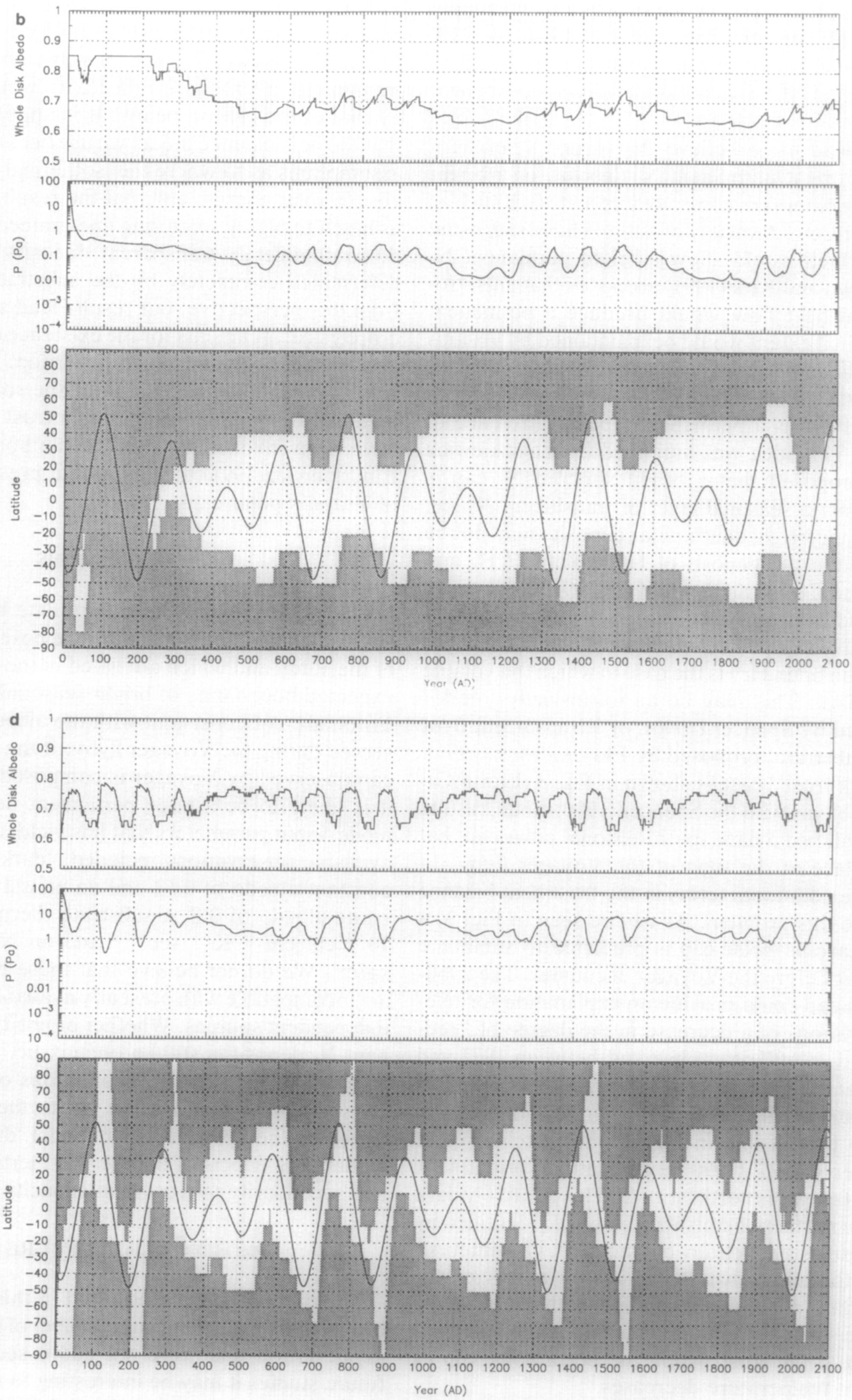

FIG. 4—*Continued*

the frost to the poles. With low thermal inertia, the model predicts a bright northern cap in place down to ~10° north latitude, which, like the north polar cap predicted by Stansberry *et al.* (1990), was not observed in the Voyager images.

Our results lead us to believe that Triton's southern cap is either a bright permanent N_2 deposit, or a bright permanent cap composed of less volatile materials such as methane and/or CO_2. A variety of authors have suggested mechanisms which would allow a bright permanent N_2 polar cap. Brown and Kirk (1991) proposed that anisotropies in internal heat flow would produce a permanent cap. Its latitudinal extent would be maintained by viscous spreading as the cap sagged under its own weight (Kirk and Brown 1991). Another possibility proposed by Moore and Spencer (1990) is a permanent albedo difference of the substrate. This idea was amplified by Eluszkiewicz (1991), who proposed that a bright sintered N_2 cap is maintained under a seasonal layer of translucent N_2 ice. Alternatively, the bright south polar deposits may not be N_2 at all, but the lag deposit of less volatile CH_4 and possibly CO and CO_2 (Grundy and Fink 1991, Cruikshank *et al.* 1991, and Trafton 1992).

A seasonal N_2 cap which yields a better match to the observed albedo boundary is the case in which the volatile is relatively dark. This may be an intrinsically "dark" frost, suggested by Spencer (1990), or a translucent frost over a dark substrate, proposed by Eluszkiewicz (1991). Our best "dark frost" case is shown in Fig. 3 (Run #33). One of the problems with the Spencer (1990) model results was that it predicted a dark south seasonal polar cap that was still in place at the time of the Voyager flyby. In our model, the additional terms in the frost heat balance equation solve this problem. As can be seen in Fig. 3, a dark south seasonal polar cap is predicted to sublimate completely just before the Voyager encounter. The sublimation of this cap could provide an explanation for telescopic observations of a decrease in the degree of "redness" of the disk of Triton observed between 1977 and 1989 (Smith *et al.* 1989). Furthermore, if one compares the albedo boundary for the forming northern dark cap in our model to that visible in Fig. 1, the match is quite good. Stansberry *et al.* (1990) also identify a bright/dark boundary at 10 degrees north latitude. This relatively dark material in the northern hemisphere was also identified by McEwen (1990) as a spectrally distinct unit. One interesting aspect of the plot shown in Fig. 3 is the nonalignment of the maximum polar cap excursion with the extreme latitude of the subsolar point. This is due to the poleward redistribution of the frost within the north polar cap as the frost-point temperature decreases.

One of the least well constrained aspects of Triton's seasonal nitrogen cycle is the microphysical nature of the nitrogen frost itself. There have been a number of studies which suggest that once deposited, N_2 frost grains undergo significant metamorphosis (Zent *et al.* 1989; Kirk 1990; Eluszkiewicz 1991), possibly forming a smooth translucent layer whose reflectivity would be dominated by that of the ground below. It is important to point out that the heat balance model we use here makes no specific assumptions as to where the isothermal N_2 frost deposits absorb solar energy, and that the results we quote apply as much to highly scattering fine-grained deposits as they do to completely transparent deposits whose albedo is determined completely by the substrate. When viewed from this perspective, our results lend support to the microphysical arguments for the existence of "dark," nearly transparent N_2 frost deposits on Triton. Furthermore, our results obviate the necessity for the somewhat arbitrary large-scale temporal variations in frost reflectivities that have been invoked by previous authors (Spencer 1990, Eluszkiewicz 1991) to explain the present configuration of Triton's polar caps.

CONCLUSIONS

The model results obtained to date have provided answers to many of the questions we posed at the beginning of the study and which are listed in the introduction. The expected boundaries of bright seasonal N_2 polar caps on Triton are not consistent with the albedo boundaries observed during the Voyager flyby. If the bright south polar cap observed by Voyager is composed of solid N_2, then it is likely to be a large permanent deposit. The set of model input parameters that has yielded the best fit to the available observations included "dark" N_2 frost with a constant albedo of 0.62 and an emissivity of 0.5, a substrate albedo of 0.8, a substrate thermal inertia of 7×10^{-3} cal cm^{-2} K^{-1} sec$^{-1/2}$ and an N_2 inventory of 50 kg/m^2. We do not believe that these best-fit parameters are incompatible with presently available constraints from independent sources. Whether or not Triton has a permanent N_2 deposit is still an open issue. The model results also predict that climatic conditions on Triton can vary considerably with time, but not to the same extent predicted by the Spencer (1990) model, due primarily to the moderating effects of the thermal inertia of the substrate, and secondarily to frost heat capacity.

PROSPECTS FOR FUTURE WORK

The thermal model described in this paper is likely to be of value for considering a number of scientific questions about Triton that were not addressed in this study. In future studies it may be interesting to model the seasonal cycles of CH_4 and CO, to investigate whether the bright south polar cap could have been composed of these two ices.

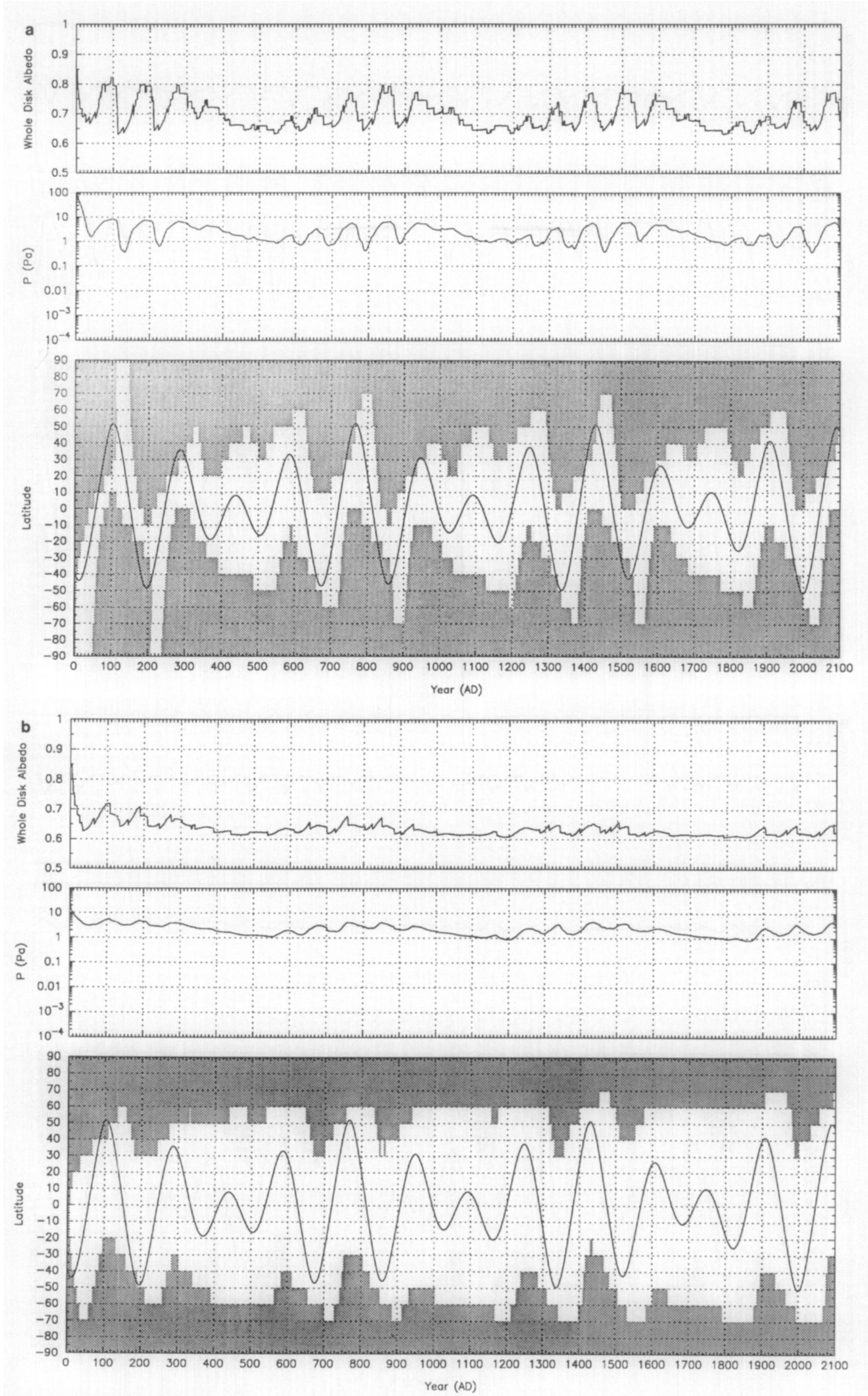

FIG. 5. These two cases show the effect of changing thermal inertia while frost albedo, emissivity, and nitrogen inventory are held constant at 0.85, 0.4, and 100 kg/m^2, resp. Run #30 (a) has a low thermal inertia of 1×10^{-3} cal cm^{-2} K^{-1} sec$^{-1/2}$, and Run #35 (b) has a high thermal inertia of 20×10^{-3} cal cm^{-2} K^{-1} sec$^{-1/2}$. For these bright frost runs the higher the thermal inertia is, the less frost condenses in equatorial regions.

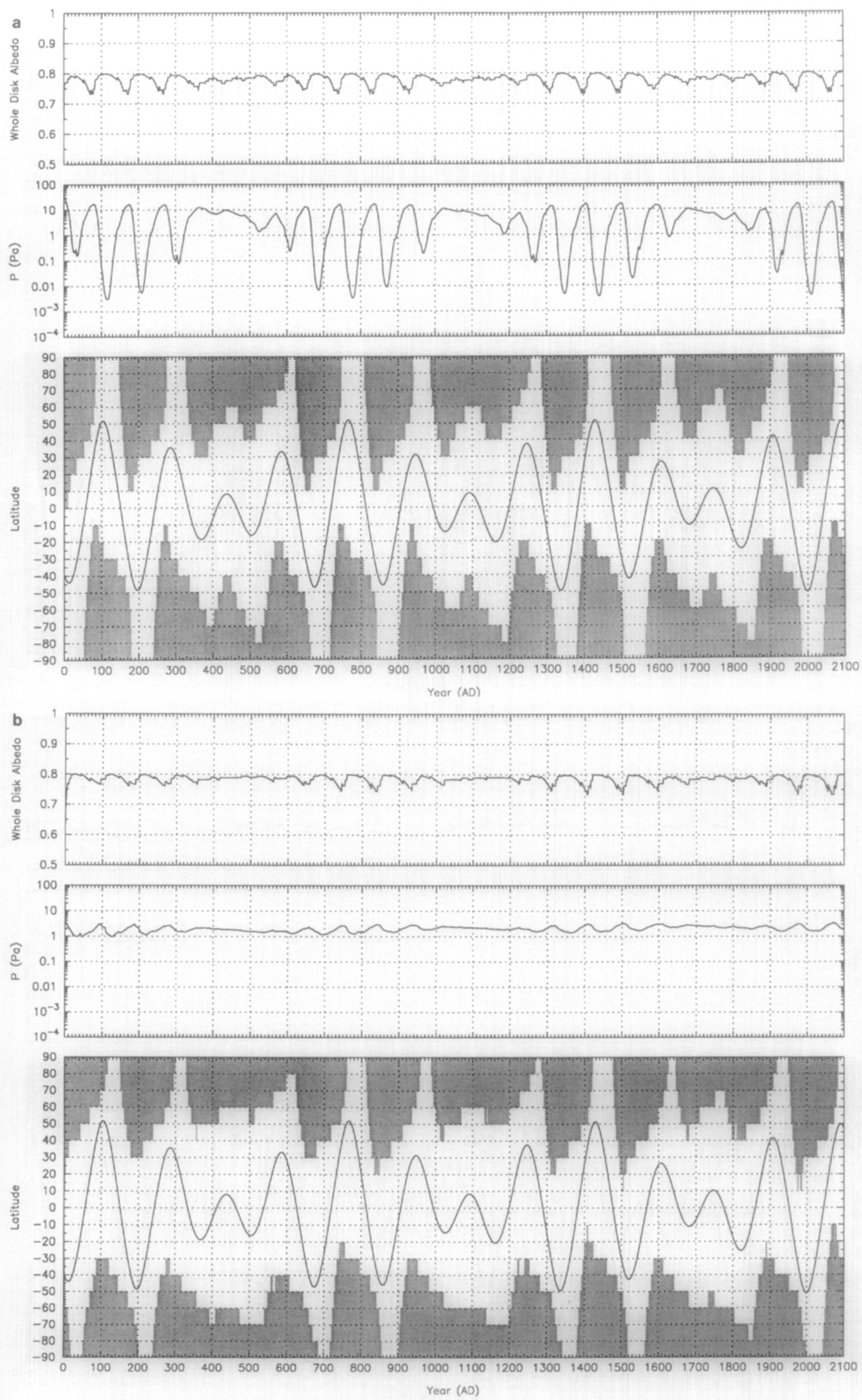

FIG. 6. These two cases show the stabilizing effect of high thermal inertia on atmospheric pressure for two dark frost runs. Run #32 (a) has a thermal inertia of 1×10^{-3} cal cm^{-2} K^{-1} sec$^{-1/2}$, and Run #34 (b) has a thermal inertia of 50×10^{-3} cal cm^{-2} K^{-1} sec$^{-1/2}$. Both cases have an emissivity of 0.5 and an N_2 inventory of 50 kg/m^2. Thermal inertia has only a minor effect on polar cap boundaries in dark frost cases, but the trend (to clear out the equatorial region as the thermal inertia increases) is the same as for the bright frost cases.

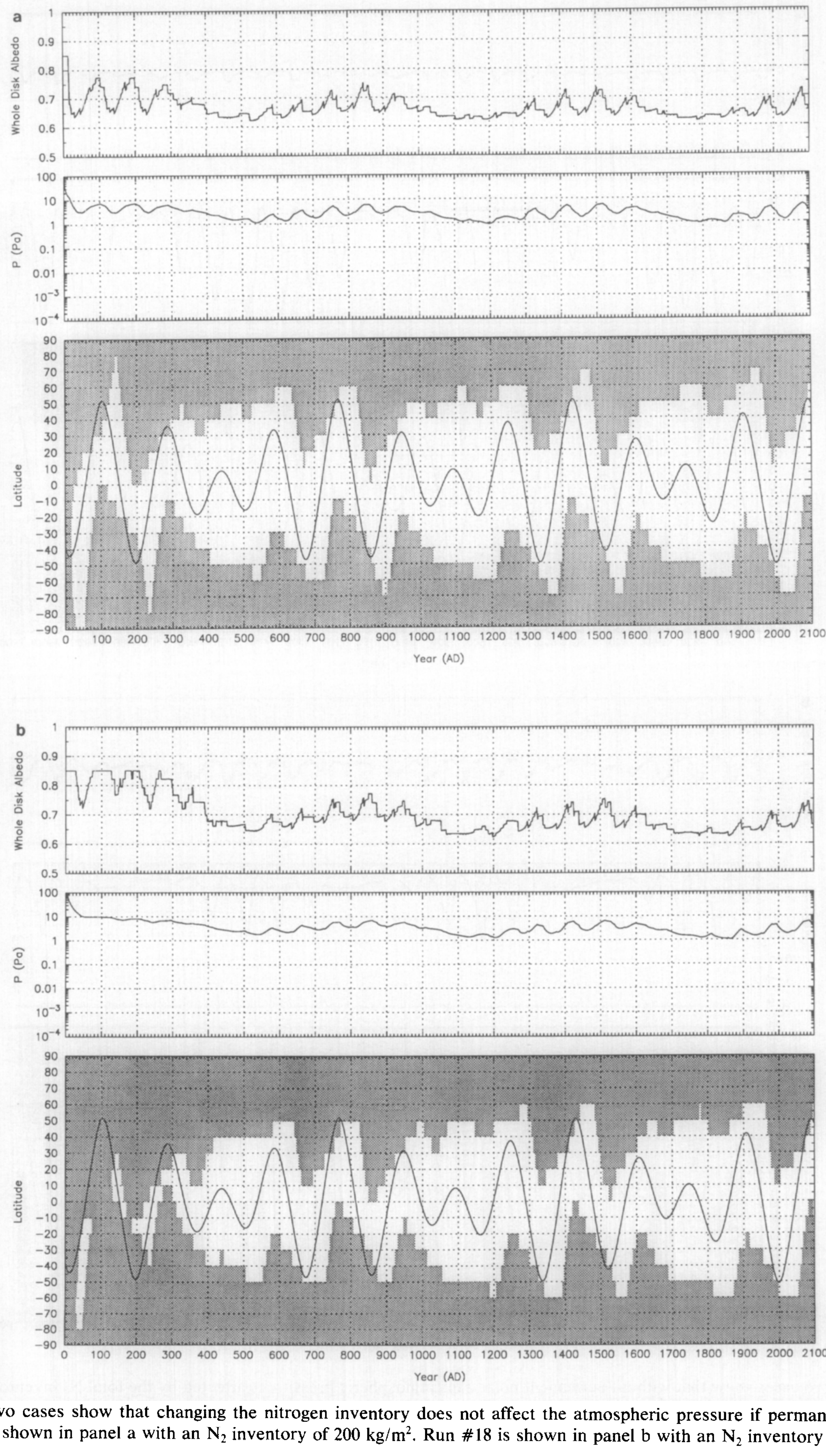

FIG. 7. These two cases show that changing the nitrogen inventory does not affect the atmospheric pressure if permanent polar caps are present. Run #31 is shown in panel a with an N_2 inventory of 200 kg/m^2. Run #18 is shown in panel b with an N_2 inventory of 100 kg/m^2.

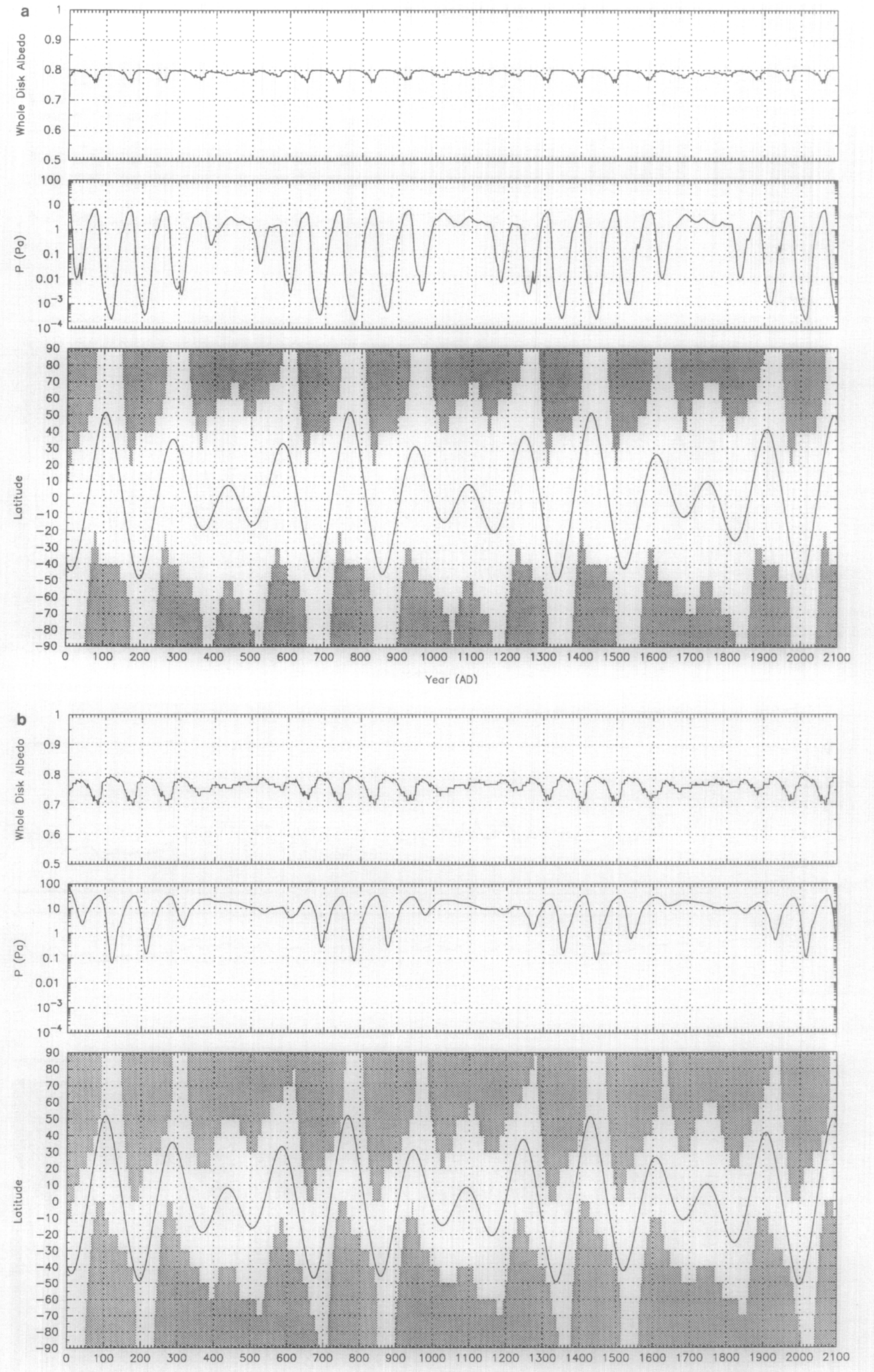

FIG. 8. These two cases show that without permanent polar caps atmospheric pressure is affected by the total N_2 inventory. Panel a (run #2) compares an N_2 inventory of 20 kg/m^2 with an inventory of 100 kg/m^2 shown in panel b (run #53).

In addition to the limited number of observable quantities considered here, there also exist a set of aeolian markers identified in the Voyager images by Ingersoll (1990) and Hansen *et al.* (1990). These data could be used in conjunction with coupled surface–atmosphere models to investigate diurnal and seasonal volatile transport on Triton and its effect on atmospheric dynamics.

The present model can also be refined further to account for the possibility of vertical temperature gradients within seasonal nitrogen frost deposits during freeze-out conditions, temporally variable frost properties, latitudinal variations in the heat flow rate, and the behavior of the Triton cap–atmosphere system over longer timescales, including other processes that may redistribute solid N_2. It is also likely that future laboratory and telescopic observations will yield additional constraints on the composition and physical properties of Triton surface materials. Such new information could potentially result in a significant reduction in the present volume of "Triton parameter space," and would make it possible to use thermal models like the one employed here to place even stronger constraints on the nature and behavior of Triton's polar caps. Finally, observations of the north polar region will be achievable in AD 2080.

ACKNOWLEDGMENTS

Very helpful comments were received from Andrew Ingersoll, Jonathan Lunine, Robert Nelson, John Spencer, and an anonymous reviewer. The research described in this paper was carried out at the Jet Propulsion Laboratory, California Institute of Technology, under a contract with the National Aeronautics and Space Administration, under the auspices of the Neptune Data Analysis Program.

REFERENCES

BROADFOOT, L., S. ATREYA, J. BERTAUX, J. BLAMONT, A. DESSLER, T. DONAHUE, W. FORRESTER, D. HALL, F. HERBERT, J. HOLBERG, D. HUNTEN, V. KRASNOPOLSKY, S. LINICK, J. LUNINE, J. MCCONNELL, H. MOOS, B. SANDEL, N. SCHNEIDER, D. SHEMANSKY, G. SMITH, D. STROBEL, AND R. YELLE (1989). Ultraviolet spectrometer observations of Neptune and Triton. *Science* **246,** 1459–1465.

BROWN, G. N., AND W. T. ZIEGLER (1980). Vapor pressure and heats of vaporization and sublimation of liquids and solids of interest in cryogenics below 1-atm pressure. *Adv. Cryogen. Engng.* **25,** 662–670.

BROWN, R. H., T. JOHNSON, J. GOGUEN, G. SCHUBERT, AND M. ROSS (1991). Triton's global heat budget. *Science* **251,** 1465–1467.

BROWN, R. H., AND R. L. KIRK (1991). Coupling of internal heat to volatile transport on Triton. *Bull. Am. Astron. Soc.* **23,** 1210.

CLIFFORD, S. M., AND C. J. BARTELS (1986). The Mars thermal model (MARSTHERM): A Fortran 77 finite difference thermal model designed for general distribution. *Lunar Planet. Sci.* **17,** 142–143.

CONRATH, B., F. FLASAR, R. HANEL, V. KUNDE, W. MAGUIRE, J. PEARL, J. PIRRAGLIA, R. SAMUELSON, P. GIERRASCH, A. WEIR, B. BEZARD, D. GAUTIER, D. CRUIKSHANK, L. HORN, R. SPRINGER, AND W. SHAFFER (1989). Infrared observations of the Neptunian system. *Science* **246,** 1454–1459.

CRUIKSHANK, D., AND J. APT (1984). Methane on Triton: Physical state and distribution. *Icarus* **58,** 306–311.

CRUIKSHANK, D., R. H. BROWN, AND R. CLARK (1984). Nitrogen on Triton. *Icarus* **58,** 293–305.

CRUIKSHANK, D., R. BROWN, L. GIVER, AND A. TOKUNAGA (1989). Triton: Do we see to the surface? *Science* **245,** 283–289.

CRUIKSHANK, D., T. OWEN, T. GEBALLE, B. SCHMITT, C. DEBERGH, J-P. MAILLARD, B. LUTZ, AND R. BROWN (1991). Tentative detection of CO and CO_2 ices on Triton. *Bull. Am. Astron. Soc.* **23,** 1208.

ELUSZKIEWICZ, J. (1991). On the microphysical state of the surface of Triton. *J. Geophys. Res.* **96,** 217–231.

GRUNDY, W. M., AND U. FINK (1991). A new spectrum of Triton near the time of the Voyager encounter. *Icarus* **93,** 379–385.

HANSEN, C., A. MCEWEN, A. INGERSOLL, AND R. TERRILE (1990). Surface and airborne evidence for plumes and winds on Triton. *Science* **250,** 421–424.

HANSEN, C., AND D. PAIGE (1991) A Triton thermal model. *Bull. Am. Astron. Soc.* **23,** 1208.

HARRIS, A. (1984). *Physical Properties of Neptune and Triton Inferred from the Orbit of Triton.* NASA Conference Publication 2330.

INGERSOLL, A. (1990). Dynamics of Triton's atmosphere. *Nature* **344,** 315–317.

JAKOSKY, B. M., AND R. M. HABERLE (1990). Year to year instability of the Mars south polar cap. *J. Geophys. Res.* **84,** 2923–2927.

JOHNSON, V., Ed. (1960). *A Compendium of the Properties of Materials at Low Temperature (Part 1).* Wadd Technical Report 60-56.

KIRK, R. L. (1990). Diffusion kinetics of solid methane and nitrogen: Implications for Triton. *Lunar Planet. Sci.* **21,** 631–632.

KIRK, R. L., AND R. H. BROWN (1991). Models of the viscous spreading of Triton's permanent polar caps. *Bull. Am. Astron. Soc.* **23,** 1209.

LEIGHTON, R., AND B. MURRAY (1966). Behavior of carbon dioxide and other volatiles on Mars. *Science* **153,** 136–144.

MCEWEN, A. (1990). Global color and albedo variations on Triton. *Geophys. Res. Lett.* **17,** 1765–1768.

MOORE, J. M., AND J. R. SPENCER (1990). Koyaanismuuyaw: The hypothesis of a perenially dichotomous Triton. *Geophys. Res. Lett.* **17,** 1757–1760.

MORRISON, D., AND D. P. CRUIKSHANK (1973). Thermal properties of the Galilean satellites. *Icarus* **18,** 224–236.

MURRAY, B. C., AND M. C. MALIN (1973). Polar volatiles on Mars—Theory versus observation. *Science* **182,** 437–443.

NELSON, R. M., W. D. SMYTHE, B. D. WALLIS, L. J. HORN, A. L. LANE, AND M. J. MAYO (1990). Temperature and thermal emissivity of the surface of Neptune's satellite Triton. *Science* **250,** 429–431.

PAIGE, D. A. (1992). The thermal stability of near-surface ground ice on Mars. *Nature* **356,** 43–45.

PAIGE, D. A., AND S. E. WOOD (1992). Modeling the Martian seasonal CO_2 cycle. 2. Interannual variability. *Icarus* **100,** 15–28.

SMITH, B., L. SODERBLOM, D. BANFIELD, C. BARNET, A. BASILEVSKY, R. BEEBE, K. BOLLINGER, J. BOYCE, A. BRAHIC, G. BRIGGS, R. H. BROWN, C. CHYBA, S. COLLINS, T. COLVIN, A. COOK II, D. CRISP, S. CROFT, D. CRUIKSHANK, J. CUZZI, G. DANIELSON, M. DAVIES, E. DEJONG, L. DONES, D. GODFREY, J. GOGUEN, I. GRENIER, V. HAEMMERLE, H. HAMMEL, C. HANSEN, P. HELFENSTEIN, C. HOWELL, G. HUNT, A. INGERSOLL, T. JOHNSON, J. KARGEL, R. KIRK, D. KUEHN, S. LIMAYE, H. MASURSKY, A. MCEWEN, D. MORRISON, T. OWEN, W. OWEN, J. POLLACK, C. PORCO, K. RAGES, P. ROGERS, D. RUDY, C. SAGAN, J. SCHWARTZ, E. SHOEMAKER, M. SHOWALTER, B. SECARDY, D. SIMONELLI, J. SPENCER, L. SROMOVSKY, C. STOKER, R. STROM, V. SUOMI, S. SYNNOTT, R. TERRILE, P. THOMAS, W.

THOMPSON, A. VERBISCER, AND J. VEVERKA (1989). Voyager 2 at Neptune: Imaging science results. *Science* **246,** 1422–1450.

SPENCER, J. (1990). Nitrogen frost migration on Triton: A historical model. *Geophys. Res. Lett.* **17,** 1769–1772.

SPENCER, J., AND J. MOORE (1992). The influence of thermal inertia on temperatures and frost stability on Triton. *Icarus* **99,** 261–272.

STANSBERRY, J., J. LUNINE, AND C. PORCO (1990). Zonally averaged thermal balance and stability models for nitrogen polar caps on Triton. *Geophys. Res. Lett.* **17,** 1773–1776.

TRAFTON, L. (1984). Large seasonal variations in Triton's atmosphere. *Icarus* **58,** 312–324.

TRAFTON, L. M. (1992). Methane enhancement in Triton's south polar cap: Interpretation in terms of CH_4 and N_2 in solid solution. Neptune and Triton Conference Abstract.

TYLER, G., D. SWEETNAM, J. ANDERSON, S. BORUTZKI, J. CAMPBELL, V. ESHLEMAN, D. GRESH, E. GURROLA, D. HINSON, N. KAWASHIMA, E. KURSINSKI, G. LEVY, G. LINDAL, J. LYONS, E. MAROUF, P. ROSEN, R. SIMPSON, AND G. WOOD (1989). Voyager radio science observations of Neptune and Triton. *Science* **246,** 1466–1473.

WOOD, S. E., AND D. A. PAIGE (1992). Modeling the Martian seasonal CO_2 cycle. 1. Fitting the Viking lander pressure curves. *Icarus* **100,** 1–14.

YELLE, R. V. (1992). The effect of surface roughness on Triton's volatile distribution. *Science* **255,** 1–3.

ZENT, A. P., C. P. MCKAY, J. B. POLLACK, AND D. P. CRUIKSHANK (1989). Grain metamorphism in polar nitrogen ice on Triton. *Geophys. Res. Lett.* **16,** 965–969.